LLNL-TR-741445

LAWRENCE
LIVERMORE
NATIONAL
LABORATORY

# M4SF-17LL010302072: The Roles of Diffusion and Corrosion in Radionuclide Retardation

M. Zavarin, E. Balboni, C. Atkins-Duffin

November 9, 2017

## Disclaimer

This work performed under the auspices of the U.S. Department of Energy by Lawrence Livermore National Laboratory under Contract DE-AC52-07NA27344.

# Appendix E
# FCT Document Cover Sheet

Name/Title of Deliverable/Milestone: M4SF-17LL010302072: The Roles of Diffusion and Corrosion in Radionuclide Retardation

Work Package Title and Number: M4SF-17LL01030207 DR Crystalline Disposal R&D - LLNL

Work Package WBS Number: 1.02.08.01.03.02

Responsible Work Package Manager: Mavrik Zavarin

(Name/Signature)

Date Submitted

| | | | | |
|---|---|---|---|---|
| Quality Rigor Level for Deliverable/Milestone | ☒ QRL-3 | ☐ QRL-2 | ☐ QRL-1<br>☐ Nuclear Data | ☐ N/A* |

This deliverable was prepared in accordance with Lawrence Livermore National Laboratory's QA program which meets the requirements of

☒ DOE Order 414.1　　☐ NQA-1-2000

**This Deliverable was subjected to:**

| | |
|---|---|
| ☒ Technical Review | ☐ Peer Review |
| **Technical Review (TR)** | **Peer Review (PR)** |
| **Review Documentation Provided** | **Review Documentation Provided** |
| ☐ Signed TR Report or, | ☐ Signed PR Report or, |
| ☐ Signed TR Concurrence Sheet or, | ☐ Signed PR Concurrence Sheet or, |
| ☒ Signature of TR Reviewer(s) below | ☐ Signature of PR Reviewer(s) below |

**Name and Signature of Reviewers**

| | |
|---|---|
| Brian L. Anderson | Brian L. Anderson |
| Gregory Pope | |

*Note: In some cases there may be a milestone where an item is being fabricated, maintenance is being performed on a facility, or a document is being issued through a formal document control process where it specifically calls out a formal review of the document. In these cases, documentation (e.g., inspection report, maintenance request, work planning package documentation or the documented review of the issued document through the document control process) of the completion of the activity along with the Document Cover Sheet is sufficient to demonstrate achieving the milestone. QRL for such milestones may be also be marked N/A in the work package provided the work package clearly specifies the requirement to use the Document Cover Sheet and provide supporting documentation.

## Appendix E
## FCT Document Cover Sheet

| | |
|---|---|
| Name/Title of Deliverable/Milestone | M4SF-17LL010302072: The Roles of Diffusion and Corrosion in Radionuclide Retardation |
| Work Package Title and Number | M4SF-17LL01030207 DR Crystalline Disposal R&D - LLNL |
| Work Package WBS Number | 1.02.08.01.03.02 |
| Responsible Work Package Manager | Mavrik Zavarin<br>(Name/Signature) |
| Date Submitted | |

| | | | | |
|---|---|---|---|---|
| Quality Rigor Level for Deliverable/Milestone | ☒ QRL-3 | ☐ QRL-2 | ☐ QRL-1<br>☐ Nuclear Data | ☐ N/A* |

This deliverable was prepared in accordance with Lawrence Livermore National Laboratory's QA program which meets the requirements of

☒ DOE Order 414.1 ☐ NQA-1-2000

**This Deliverable was subjected to:**

| | |
|---|---|
| ☒ Technical Review | ☐ Peer Review |
| **Technical Review (TR)** | **Peer Review (PR)** |
| **Review Documentation Provided** | **Review Documentation Provided** |
| ☐ Signed TR Report or, | ☐ Signed PR Report or, |
| ☐ Signed TR Concurrence Sheet or, | ☐ Signed PR Concurrence Sheet or, |
| ☒ Signature of TR Reviewer(s) below | ☐ Signature of PR Reviewer(s) below |

**Name and Signature of Reviewers**

| | |
|---|---|
| Brian L. Anderson | |
| Gregory Pope | Gregory Pope |

*Note: In some cases there may be a milestone where an item is being fabricated, maintenance is being performed on a facility, or a document is being issued through a formal document control process where it specifically calls out a formal review of the document. In these cases, documentation (e.g., inspection report, maintenance request, work planning package documentation or the documented review of the issued document through the document control process) of the completion of the activity along with the Document Cover Sheet is sufficient to demonstrate achieving the milestone. QRL for such milestones may be also be marked N/A in the work package provided the work package clearly specifies the requirement to use the Document Cover Sheet and provide supporting documentation.

LAWRENCE
LIVERMORE
NATIONAL
LABORATORY

LLNL-TR-741445

# M4SF-17LL010302072: The Roles of Diffusion and Corrosion in Radionuclide Retardation

M. Zavarin, E. Balboni, C. Atkins-Duffin

September 21, 2017

## Disclaimer

This work performed under the auspices of the U.S. Department of Energy by Lawrence Livermore National Laboratory under Contract DE-AC52-07NA27344.

**September 5, 2017**

# M4SF-17LL010302072: The Roles of Diffusion and Corrosion in Radionuclide Retardation

**M. Zavarin, E. Balboni, Cindy Atkins-Duffin**

Glenn T. Seaborg Institute, Physical & Life Sciences, Lawrence Livermore National Laboratory, 7000 East Avenue, Livermore, CA 94550, USA.

# Contents

# 1. Introduction

This progress report (Level 4 Milestone Number M4SF-17LL010302072) summarizes research conducted at Lawrence Livermore National Laboratory (LLNL) within the Crystalline Disposal R&D Activity Number M4SF-17LL01030207 and Crystalline International Collaborations Activity Number M4SF-17LL01030208. The focus of this research is the interaction of radionuclides with Engineered Barrier System (EBS) and host rock materials at various physico-chemical conditions relevant to subsurface repository environments. They include both chemical and physical processes such as solubility, sorption, and diffusion.

LLNL is supporting the overall objectives of the DR Crystalline Disposal R&D control account. The objective of this control account is to advance our understanding of long-term disposal of spent fuel in crystalline rocks (including both granitic and metamorphic rocks) and to develop necessary experimental and computational capabilities to evaluate various disposal concepts in such media. The objectives of this work package are to conduct experimental and modeling studies to quantify radionuclide diffusion through bentonite under repository-relevant (reducing) conditions and to quantify radionuclide sequestration as a result of canister breaching and near field corrosion processes.  Quantification of these processes will be included in the GDSA model. A basic ‘minimal’ process model for radionuclide diffusion and corrosion-enhanced radionuclide sequestration processes will be provided to GDSA to support a 2020 repository performance assessment schedule.

In FY17, LLNL continued their efforts in data collection and model development in support of the SFWST program.  In particular, our research focused on identification, quantification, and parameterization of processes relevant for the evaluation of the performance of various repository scenarios under investigation by the SFWST program.

Our specific FY17 goals for the crystalline work package were the following:

- Completion of the Np(IV) diffusion experiments and quantification of the diffusion rates in bentonite backfill material.
- Evaluation of the radionuclide sequestration potential of corrosion products produced during canister breaching and radionuclide release

Our interest in radionuclide sequestration by corrosion products stems from (1) the potential for this process to significant inhibit radionuclide release during canister breaching and (2) from the absence of such processes in most repository performance assessments. Discussions with James Jerden (Argonne National Laboratory) suggest that a model of radionuclide incorporation can be added to the waste package cell of the GDSA model and may lead to a reduction in the source term of mobile radionuclides. Steel corrosion rates have been implemented within the spent fuel matrix degradation process model but have not yet been implemented into GDSA.  Results from an experimental and modeling study of radionuclide partitioning into steel corrosion products will facilitate the incorporation of this process into the GDSA as the steel corrosion model is implemented.

LLNL evaluated this process from both an experimental and modeling perspective. Experimentally, LLNL has been in the process of developing methodologies to grow various iron oxides phases (goethite, hematite, magnetite) in the presence of radionuclides. We performed a small number of binary (RN-mineral) coprecipitation experiments to test radionuclide (Pu, Am, Np, and U) partitioning.  Experiments are attempting to quantify coprecipitation partitioning and also examine the effects of aging and the potential iron oxide recrystallization effects associated with the presence of aqueous phase Fe(II).

LLNL is also supporting the overall objectives of the DR Crystalline International R&D control account. The Crystalline International work package is focused on identifying beneficial international partner programs that can facilitate the development of US GDSA models and ensure that repository development is performed using internationally recognized state of the art methodologies. Therefore, this work contributes to the GDSA model activities by providing parameter feeds and support requirements for the capability for a robust repository performance assessment model by 2020.

LLNL's contribution with this control account is summarized, in part, in the Crystalline and Argillite work packages. Specifically, LLNL efforts will be focused on the following:

- Continued engagement with the NEA TDB project through the support of Dr. Atkins-Duffin as the SFWST representative for international thermodynamic database development effort. This effort ensures that US GDSA model efforts are aligned with internationally accepted practices for repository performance assessment calculations.
- Continued collaboration with HZDR thermodynamic and sorption database development groups in support of the database needs of the SFWST program
- Completion of a state of the art manuscript regarding colloid facilitated transport in the context of nuclear waste repositories. A report was prepared in FY16. This report will provide the basis for 1) preparing a manuscript and 2) development of a colloid facilitated transport model for use in GDSA.

In this report, we summarize the results of two specific activities that fall under this level 4 Milestone: A summary of LLNL's engagement with NEA-TDB activities and a description of experiments performed as part of the canister corrosion and radionuclide sequestration study.

## 2. Engagement with NEA-TDB activities

On April 11, 2017, the NEA-TDB Executive Group presided over a Workshop on the Future of the Thermochemical Database (TDB) Project – Phase 6. The workshop was intended to discuss the interest of the international community in continuing the TDB effort into a Phase 6 (Phase 5 was intended to be complete in FY17). As part of the workshop, the executive committee invited international participation in the workshop. Mavrik Zavarin, Carlos Jove-Colon, and Cindy Atkins-Duffin all participated in the workshop discussions.

Prior to the workshop, Mavrik Zavarin and Carlos Jove-Colon prepared answers to a questionnaire that was distributed by the executive committee to the international community. The questionnaire was intended to help identify the need for a Phase 6 activity and the priority research areas associated with the Phase 6 activity. There was overwhelming consensus that the NEA-TDB project remains an important asset to the international nuclear waste research community. The answers to the questionnaire revealed a widely shared acknowledgement of benefit from the TDB project. This was attributed "to (*i*) the high-quality core of values provided, that are used as a basis for the organizations to complete and use according to their individual needs, (*ii*) the detailed guidelines, and (*iii*) the study of common topics of interest.

The importance of centralizing thermodynamic datasets to a common point of reference was also pointed out as a benefit from the Project and as means to lower the cost of more numerous separate studies." The workshop also revealed some potential for improvements in the project, particularly from the standpoint of scheduling, timely electronic access to data, and responsiveness to specific needs of the NEA-TDB member states.

The workshop and associated questionnaire revealed the interest by the member states for the NEA-TDB's highest priority to remain the critical review of thermodynamic data relevant to the international nuclear waste repository research needs.

On April 12, 2017, The NEA-TDB Executive Group held its Eighth Meeting of the NEA TDB-5 Project. At the meeting, the status of the Blue Book critical reviews and State of the Art Reports was discussed. In addition, a new NEA-TDB electronic database for thermodynamic data was described; the electronic database feature will become available later in the year.

# 3. Corrosion: Plutonium Interaction with Iron Oxides

For the long-term performance assessment of nuclear waste repositories, knowledge about the interactions of actinide ions with mineral surfaces is imperative. Iron (oxy)hydroxides are common soil minerals and are present in intermediate level radioactive waste (Marshall et al., 2014). They also form as corrosion products of steel which is a primary structural component of a nuclear repository and of waste canister materials (Music et al., 1993). Studies have shown that Pu(IV) has high sorption affinity for goethite and hematite surfaces at circumneutral pH (Romanchuk et al., 2011; Sanchez et al., 1985; Zhao et al., 2016). At higher concentration, Pu(IV) colloids formed on goethite may undergo a lattice distortion, due to epitaxial growth, which leads to a stronger surface binding compared to other mineral phases, such as quartz (Powell et al., 2011). Gaining a detailed understanding of the interactions between iron oxide and plutonium is key in predicting the long-term stability and mobility of plutonium in the near field of nuclear waste repositories.

The hydrous ferric oxide, ferrihydrite (FH), is a common, poorly crystalline, metastable early product of both biotic and abiotic precipitation of iron, and is a precursor to other more crystalline iron oxides such as hematite ($Fe_2O_3$) and goethite (FeOOH). Ferrihydrite crystallizes to hematite or goethite depending upon solution conditions, pH, ionic strength and temperature (Schwertmann and Cornell, 2000). The hematite and goethite formation process begins with ferrihydrite particle aggregation (Fischer and Schwertmann, 1975), followed by recrystallization within the aggregate via dissolution and reprecipitation processes that occur at the nanoscale (Combes et al., 1990). During these processes, adsorbed plutonium has the potential to become incorporated into the structure of hematite or goethite.

The goal of this project was to:

- Study sorption of Pu(IV) to ferrihydrite;
- Determine the extent and mechanisms of structural incorporation (co-precipitation) of Pu into synthetic hematite and goethite synthesized from a ferrihydrite precursor.

### 3.1 Plutonium (IV) Sorption to Ferrihydrite

For this work, 2-line ferrihydrite was produced following the synthetic method proposed by Schwertmann and Cornell (2000). Briefly 10 g of $Fe(NO_3)_3.9H_2O$ is added to 125 mL of 18MΩ $H_2O$. While stirring, approximately 110 mL of 1M KOH is added slowly until the solution pH reaches a stable value between 7 and 8. The solution is centrifuged, the supernatant removed and the solid re-suspended with 18MΩ $H_2O$. This process is repeated at least twice before transferring the solid to a 3500 MWCO SnakeSkin pleated dialysis tubing, which is left in dialysis against 18MΩ $H_2O$ water for 48 hours. The solid is then removed and suspended in a 0.1M ionic strength solution to form a 1g/L suspension. Sorption experiments were performed over the pH range of 2.5 and 9, with a Pu(IV) concentration of $10^{-10}$M. A desired aliquot of plutonium was added to each specimen to obtain the desired Pu(IV) concentration and pH was adjusted using NaOH and HCl at 0.1, 0.5, and 1M. After known time intervals, the pH was measured and an aliquot of the sample removed, centrifuged with a 3 KDa filter and analyzed by liquid scintillation counting. Samples were open to the air and no effort was made to exclude carbonate.

Our preliminary results are reported in Figure 1. 76% of Pu(IV) is sorbed onto the ferrihydrite surface at pH 2.5 within two hours of the start of the sorption experiment. At pH 6 and above the sorption (after 2 hours) is between 90-96% and equilibrium is reached within 24 hours at pH of 7 and higher. For samples equilibrated in the pH range of 2.6 and 4.4, the amount of plutonium sorbed onto ferrihydrite apparently decreases with time (Figure 1). Two factors could be contributing to this apparent desorption trend: i) oxidation of Pu(IV) to Pu(V) or Pu(VI); ii) dissolution of ferrihydrite surface at low pH. To determine if the plutonium in solution oxidizes at these pHs, an oxidation state analysis was performed. The lanthanum fluoride precipitation method was used as it allows to discriminate between reduced (III/IV) and oxidized (V/VI) plutonium. Our results (Figure 2) indicate that after 30 minutes, 40% of the plutonium left in solution at pH 2.5, and ~80-90% at pH 3 and 4, is oxidized; similar results are obtained for the same samples after one week sorption time.

This preliminary work has shown a strong affinity of Pu(IV) for the ferrihydrite surface. The sorption of Pu(IV) to ferrihydrite is fast at all pH values, however pH appears to influence sorption behavior. Whereas at pH>7, sorption reaches equilibrium in 24 hours, in the pH range of 2.5-5, some plutonium desorption occurs within a few hours from the start of the sorption experiment.

Additional experiments are needed to complete our study of Pu sorption. These include:

- Determining ferrihydrite dissolution at low pH to understand plutonium desorption behavior;
- Understanding Pu(IV) sorption to ferrihydrite in an oxygen free atmosphere.

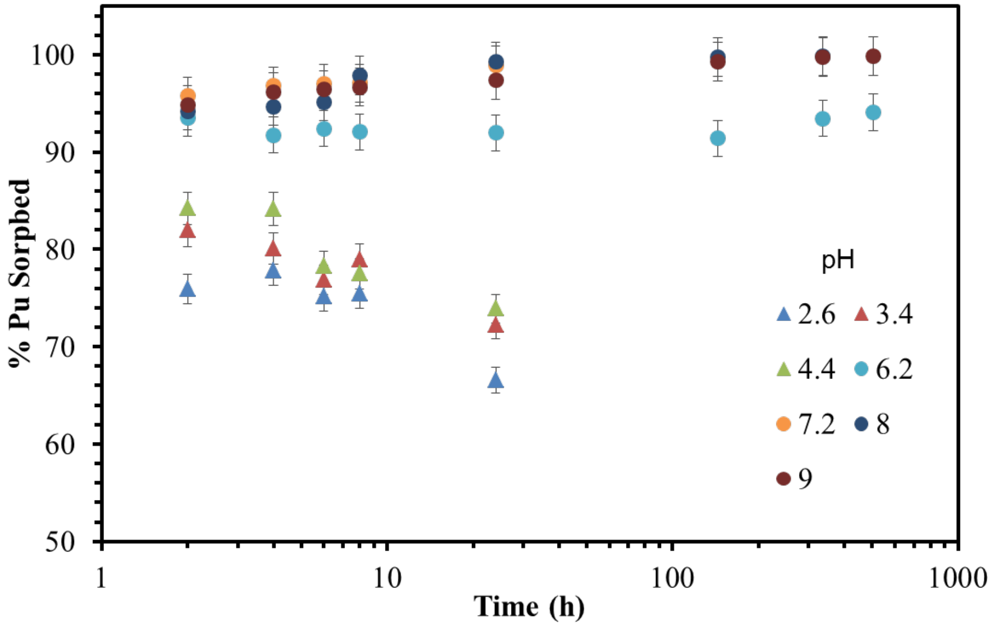

Figure 1. Sorption curve for suspended nano-particulate ferrihydrite with $10^{-10}$M Pu(IV).

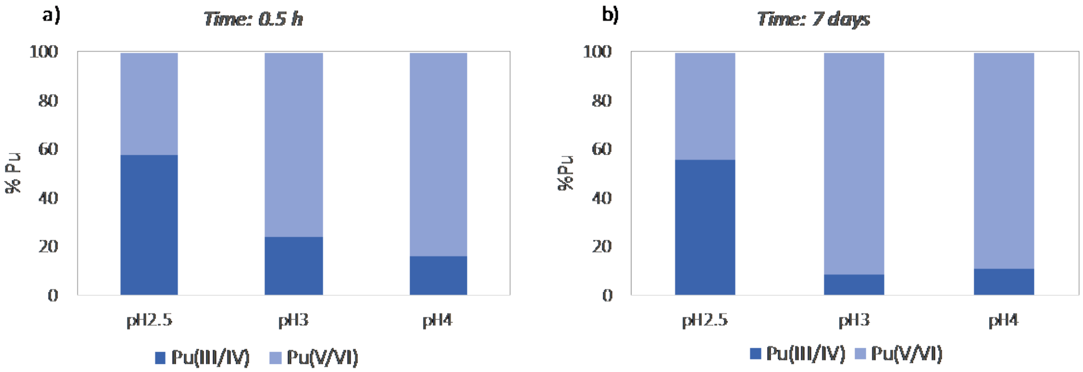

Figure 2. Oxidation state analysis of plutonium in the supernatant solution of plutonium sorption experiment on colloidal ferrihydrite a) after 30 minutes of sorption time; b) after 7 days.

## 3.2 Plutonium Coprecipitation Studies with Hematite and Goethite

Co-precipitation (or structural incorporation) of co-contaminants into mineral structures most likely involves substitution of the cation site in the mineral or perhaps interstitial incorporation. Crystal chemical constraints that affect incorporation include: i) the cation coordination environment, ii) the cation charge and, iii) a charge balancing mechanism. It has been shown that goethite and hematite are able to accommodate various impurities into their structure including Si, Ti, Mn, Ni and U(VI) (Liu et al., 2012; Marshall et al., 2014). Coprecipitation of plutonium into stable mineral phases, such as iron (oxy)hydroxides, offers a pathway for sequestration with the potential for long term immobilization.

The aim of the work was to understand:

- the difference in plutonium uptake between hematite and goethite;
- how the timing of Pu addition during goethite and hematite synthesis affect the final form of plutonium associated with these minerals.

We investigated these topics by carefully designing synthetic methodologies for both goethite and hematite and by characterizing solutions and solids of the synthesized products by a variety of analytical techniques, including liquid scintillation counting (LSC), transmission electron microscopy (TEM), powder X-ray diffraction (P-XRD), and X-ray absorption spectroscopy (XAS).

Goethite and hematite were synthesized with varying amount of plutonium (300, 1000 and 3000 ppm) from a poorly crystalline ferrihydrite (FH) precursor. The initial FH material was obtained according to the following methodologies – note that the main difference within the two synthetic pathways is the timing of plutonium addition.

- *Method A* or *coprecipitation into FH*: 1 M $FeNO_3 \cdot 9H_2O$ solution was mixed with Pu(IV), ferrihydrite was then formed by slow addition of 5 M KOH (for goethite) or 1 M KOH (for hematite);
- *Method B* or *sorption to FH method*: a KOH (5M or 1M) was slowly added to a 1M $FeNO_3.9H_2O$ solution to form ferrihydrite, Pu(IV) was then sorbed onto the ferrihydrite precipitate.

The use of either 1M KOH or 5M KOH allowed us to obtain the desired iron oxide, goethite (5M KOH) or hematite (1M KOH). The initial ferrihydrite obtained following synthetic routes "Method A" or "Method B" was aged at 80°C for 72 hours. A total of 12 samples were synthesized (Table 1).

Table 1. List of goethite and hematite samples synthesized.

| | **3000 ppm Pu** | **1000 ppm Pu** | **300 ppm Pu** |
|---|---|---|---|
| *Goethite* | | | |
| **Method A** | GA-3000 | GA-1000 | GA-300 |
| **Method B** | GB-3000 | GB-1000 | GB-300 |
| *Hematite* | | | |
| **Method A** | HeA-3000 | HeA-1000 | HeA-300 |
| **Method B** | HeB-3000 | HeB-1000 | HeB-300 |

Powder X-ray diffraction patterns of all 12 goethite and hematite samples (Table 1) aged from plutonium sorbed-on or coprecipitated into FH were collected (Figure 3). No additional peaks beyond those characteristic of the two mineral phases were identified. Figure 4 presents TEM images of samples GA-3000 and HeA-3000. Images show that goethite crystals are present as 100's of nm long and 10's of nm wide needles, banded together (Figure 4a); hematite crystals are uniform in size (50 to 60 nm) with a diamond shape (Figure 4b). These crystal morphologies are consistent with goethite and hematite crystals synthesized without plutonium as a co-contaminant. P-XRD and TEM results suggest that the addition of plutonium does not affect the final yield of the synthesis.

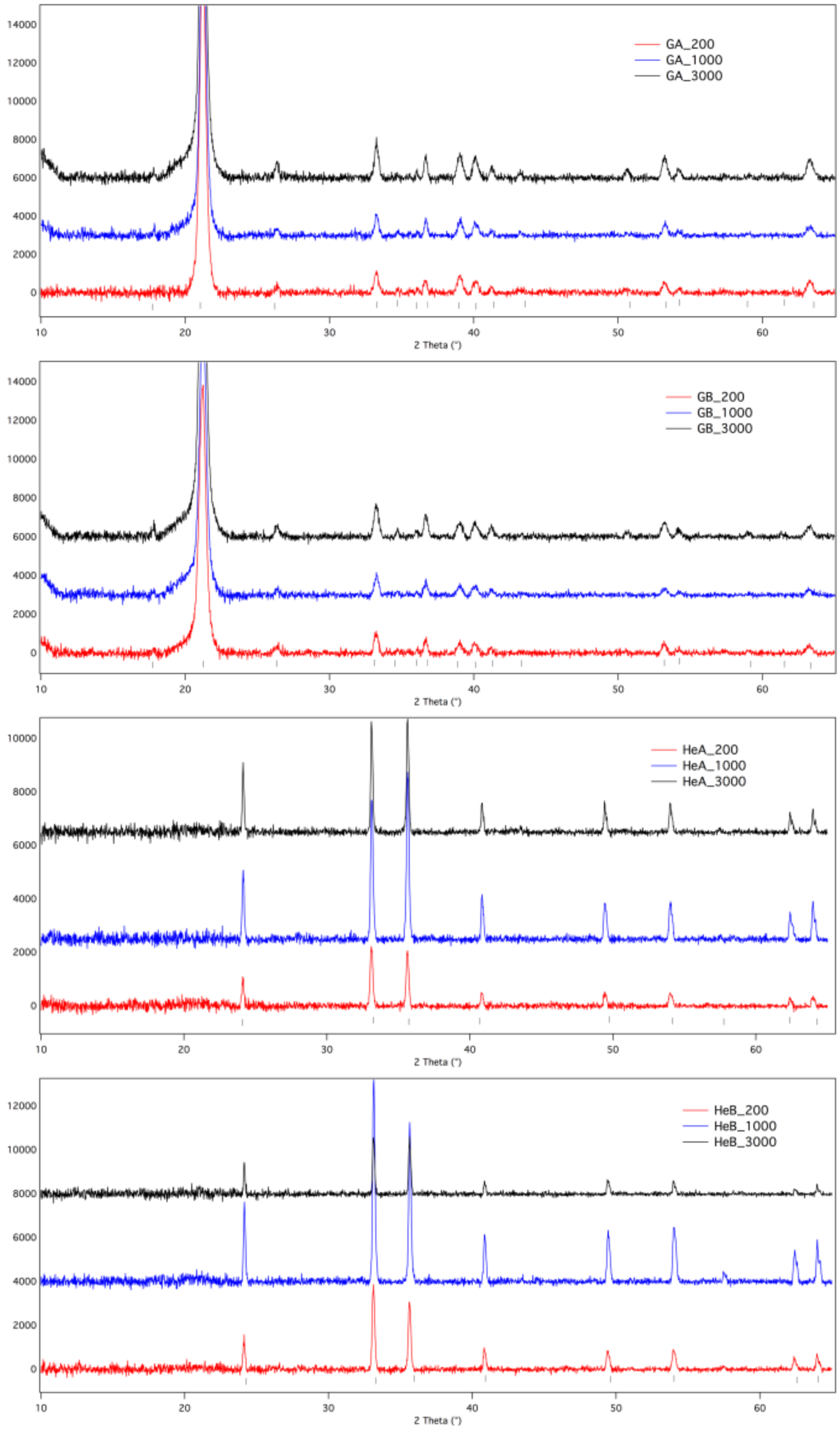

Figure 3. Powder XRD patterns of synthetic goethite (GA, GB) and hematite (HeA, HeB). PDF files to which powder XRD patterns were compared to are 00-001-0401 (goethite) and 00-002-0915 (hematite).

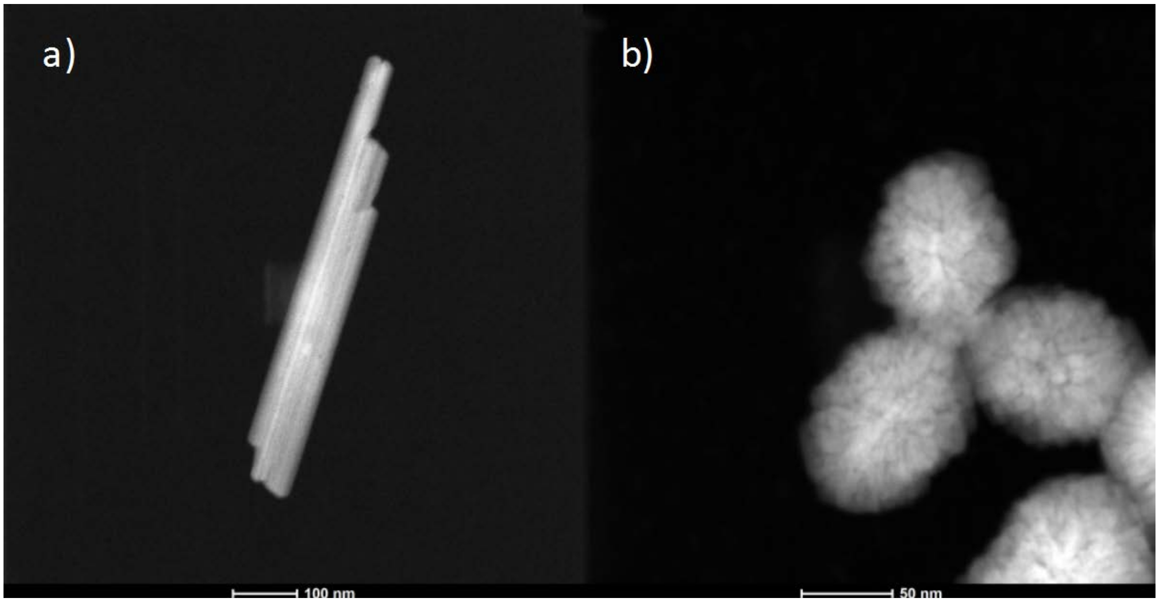

Figure 4. Scanning transmission electron microscope (STEM) image of a) goethite GA-3000 and b) hematite HeA-3000.

The fate of Pu(IV) during subsequent ferrihydrite alteration to goethite and hematite was monitored (Figure 5). For all samples, upon the completion of the synthesis (72 hours at 80°C) the plutonium concentration of the solution in contact with the mineral was measured. Solids were separated from solution by centrifugation and rinsed two times with 18MΩ $H_2O$. The plutonium concentration was measured for all rinse solutions. All plutonium concentrations were measured by liquid scintillation counting and samples were centrifuged with 3 kDa filters prior to analyses. Upon transformation of Pu(IV)–FH to goethite, 99% of the initial plutonium was associated with the solid for all samples (GA 300, 1000, 3000; GB 300, 1000, 3000 - Figure 5a). No plutonium was associated with hematite synthesized at lower plutonium concentrations (HeA 300, HeA 1000, HeB 300, HeB 1000). Only 10-20 % of plutonium was associated with the HeA 3000 and HeB 3000 samples. For all samples of goethite and hematite, the rinse solution contained < 0.01% of the initial Pu. These results suggest that Pu is strongly associated with the goethite solid, but not with hematite.

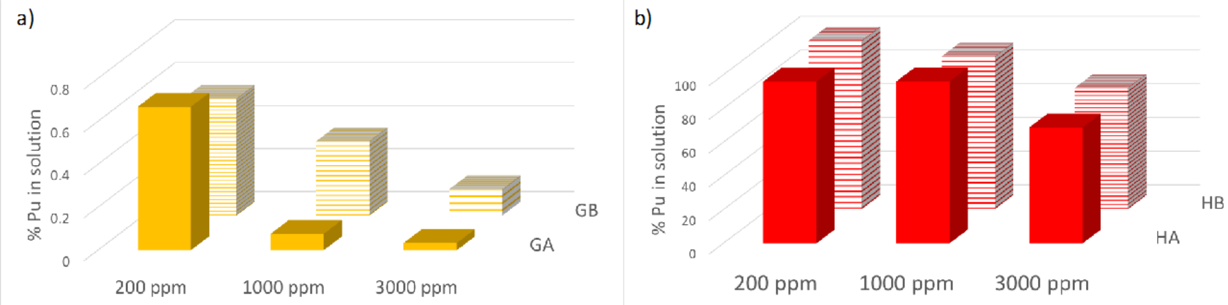

Figure 5. Plutonium measured in solution after the completion of the FH transformation to goethite (a) and hematite (b). Note y-axis on a) and b) are not to scale.

In this work, goethite and hematite were obtained using similar synthetic conditions such as chemicals used, pH and temperature and time of reaction. Differences in the extent of plutonium interaction with the two mineral phases (Figure 5) may be explained by considering the crystal chemical constraints imposed by the goethite (FeOOH) and hematite ($Fe_2O_3$) structure (Figure 6). In both minerals, there is one symmetrically independent iron site in octahedral coordination. In hematite, each Fe octahedron shares one face, two edges and three vertices with adjacent polyhedra. The edge sharing of the octahedra (Figure 6b) creates a dense (5.3g/cm$^3$) and compact structure. In goethite, each polyhedron shares three edges and three vertices with adjacent polyhedral (Figure 6c). These features together with the presence of hydroxo-groups results in a more open, less dense structure (4.2g/cm$^3$), that may be more likely to accommodate plutonium.

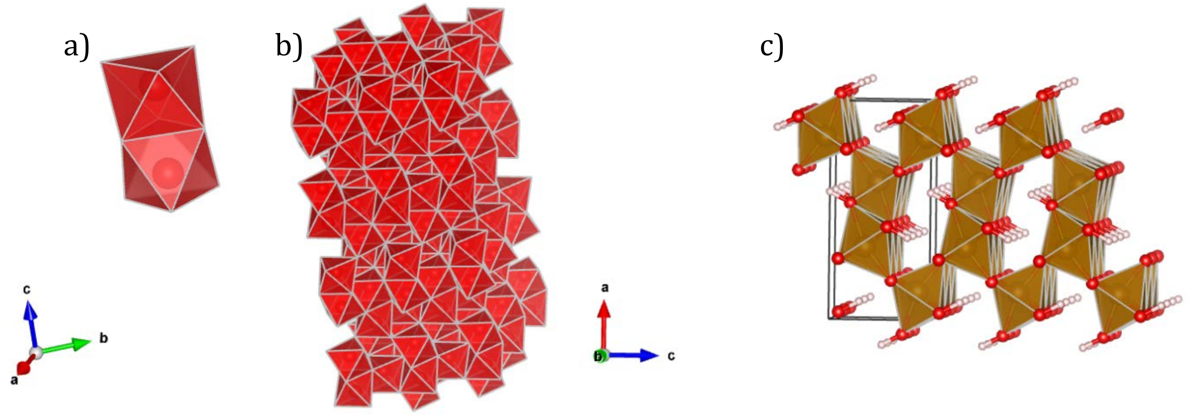

Figure 6. Polyhedral representation of the framework structure of hematite (a and b) and goethite (c). The iron coordination polyhedral are colored in red for hematite and brown for goethite.

Samples GA-3000 and GB-3000 were selected for x-ray adsorption spectroscopy (XAS) analysis at the Stanford Synchrotron Radiation Light Source (SSRL). In general, the XANES (X-ray absorption near edge structure) region of the XAS spectra provides information on oxidation state changes in the samples based on comparisons to standard reference materials. The EXAFS (extended X-ray absorption fine structure) region is fit to determine the nearby neighbors and their distances from the plutonium site.

The XANES region of the spectra confirmed that in samples GA-3000 and GB-3000 plutonium is present in the tetravalent oxidation state. However, the EXAFS spectra of samples GA-3000 and GB 3000 are different, suggesting that plutonium has different coordination environments in the two samples (Figure 7, Figure 8 and Table 2). The GB-3000 EXAFS spectrum could be fit to the model structure of $PuO_2$, with four plutonium atoms at a distance of 3.82Å (Table 2, Figure 7). This structural feature indicates that plutonium is likely present as a surface precipitate on sample GB-3000. Presence of surface bound plutonium oxides was confirmed by TEM imaging (Figure 7b). The GA-3000 spectrum could not be fit with a $PuO_2$ model. In GA-3000, plutonium is coordinated by eight oxygen atoms at 2.25(1)Å in the first coordination sphere. These bond distances are slightly shorter than the Pu-O bond distances of GB-3000, 2.31(1)Å (Table 2). In GA-3000, only two plutonium atoms could be found at distances comparable to the structure of $PuO_2$. Furthermore, an additional peak in the Fourier transform suggests that the dominant structure surrounding Pu in GA-3000 is distinct from $PuO_2$. Additional data fitting is underway to determine if the EXAFS spectra are representative of Pu substitution for Fe in the goethite structure. Nevertheless, these results clearly indicate that the timing of Pu addition in the synthetic procedures (Method A or B) affects the final form of plutonium associated with goethite.

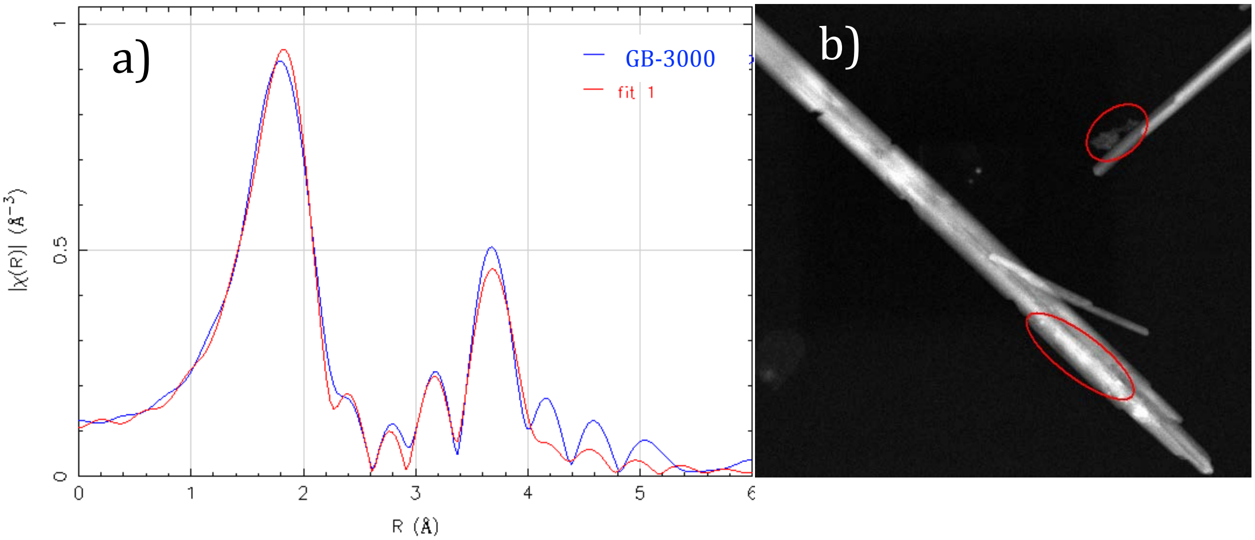

Figure 7. Fourier transforms in R (Å) of the calculated EXAFS spectra for sample GA-3000 (left) Blue line= experimental data; red line = model fit (a). STEM images of sample GB-3000, circled in red are areas of the samples where Pu surface precipitation was observed.

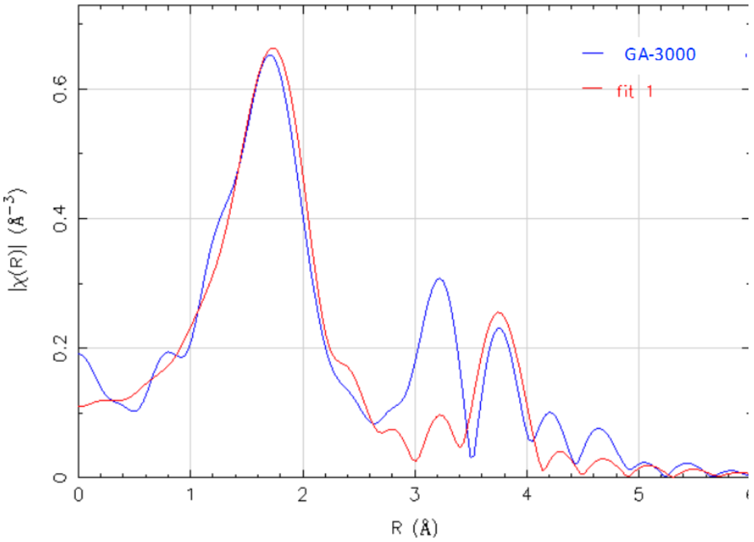

Figure 8. Fourier transforms in R (Å) of the calculated EXAFS spectra for sample GA-3000 (left) Blue line= experimental data; red line = model fit using Pu neighbors at ~3.8 Å.

Table 2. Ensemble averages of plutonium-oxygen distances and plutonium-plutonium distances in GA-3000 and GB-3000.

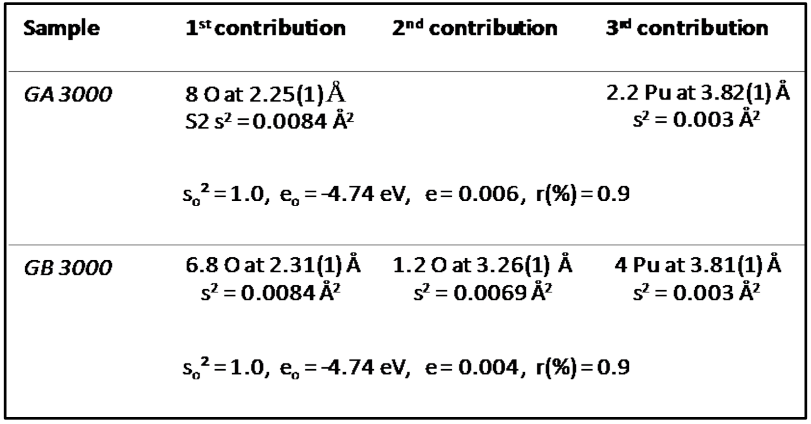

| **Sample** | **$1^{st}$ contribution** | **$2^{nd}$ contribution** | **$3^{rd}$ contribution** |
|---|---|---|---|
| *GA 3000* | 8 O at 2.25(1) Å<br>S2 $s^2 = 0.0084$ Å$^2$ | | 2.2 Pu at 3.82(1) Å<br>$s^2 = 0.003$ Å$^2$ |
| | $s_o^2 = 1.0$, $e_o = -4.74$ eV, $e = 0.006$, $r(\%) = 0.9$ | | |
| *GB 3000* | 6.8 O at 2.31(1) Å<br>$s^2 = 0.0084$ Å$^2$ | 1.2 O at 3.26(1) Å<br>$s^2 = 0.0069$ Å$^2$ | 4 Pu at 3.81(1) Å<br>$s^2 = 0.003$ Å$^2$ |
| | $s_o^2 = 1.0$, $e_o = -4.74$ eV, $e = 0.004$, $r(\%) = 0.9$ | | |

To date, our results reveal that:

- upon aging of a Pu-doped ferrihydrite precorsor into more crystalline phase, plutonium associates more strongly with goethite (FeOOH) than hematite ($Fe_2O_3$);
- the timing of Pu addition in the synthetic procedures affects the final form of plutonium associated with goethite.

## 4. Planned FY18 Efforts

In FY18, we plan to continue our efforts in data collection and model development in support of the SFWST program. Our specific FY18 goals for the crystalline and international work pages are the following:

- Completion of the Np(IV) diffusion experiments and quantification of the diffusion rates.
- Evaluation of the radionuclide sequestration potential of corrosion products produced during canister breaching and radionuclide release with an emphasis Pu incorporation into magnetite.
- Continued engagement with the NEA TDB project through the support of Dr. Atkins-Duffin as the NE representative for international thermodynamic database development effort.
- Continued collaboration with HZDR thermodynamic and sorption database development groups in support of the database needs of the UFD program

Our interest in radionuclide sequestration by corrosion products stems from (1) the potential for this process to significant inhibit radionuclide release during canister breaching and (2) from the absence of such processes in most repository performance assessments. Our FY17 experiments have revealed that Pu incorporation into iron oxides corrosion products will be controlled not only by the crystallographic form of the iron oxide but also by the timing of Pu release and iron oxide formation. A natural extension to our initial iron oxide studies is to expand into reduced forms of iron oxides that will likely predominate in a nuclear repository near field. In FY18, we will focus on synthesizing magnetite under reducing (glove box) conditions to examing the oxidation state and incorporation processes that may control Pu release under nuclear waste repository conditions.

## 5. Acknowledgments

This work was supported by the Used Fuel Disposition Campaign of the Department of Energy's Nuclear Energy Program. Prepared by LLNL under Contract DE-AC52-07NA27344.

## 6. References

Combes, J. M., Manceau, A., and Calas, G., 1990. FORMATION OF FERRIC OXIDES FROM AQUEOUS-SOLUTIONS - A POLYHEDRAL APPROACH BY X-RAY ABSORPTION-SPECTROSCOPY .2. HEMATITE FORMATION FROM FERRIC GELS. *Geochimica Et Cosmochimica Acta* **54**, 1083-1091.

Fischer, W. R. and Schwertmann, U., 1975. FORMATION OF HEMATITE FROM AMORPHOUS IRON(III)HYDROXIDE. *Clays and Clay Minerals* **23**, 33-&.

Liu, J., Liang, C., Zhang, H., Tian, Z., and Zhang, S., 2012. General Strategy for Doping Impurities (Ge, Si, Mn, Sn, Ti) in Hematite Nanocrystals. *Journal of Physical Chemistry C* **116**, 4986-4992.

Marshall, T. A., Morris, K., Law, G. T. W., Livens, F. R., Mosselmans, J. F. W., Bots, P., and Shaw, S., 2014. Incorporation of Uranium into Hematite during Crystallization from Ferrihydrite. *Environmental Science & Technology* **48**, 3724-3731.

Music, S., Gotic, M., and Popovic, S., 1993. X-RAY-DIFFRACTION AND FOURIER-TRANSFORM INFRARED-ANALYSIS OF THE RUST FORMED BY CORROSION OF STEEL IN AQUEOUS-SOLUTIONS. *Journal of Materials Science* **28**, 5744-5752.

Powell, B. A., Dai, Z., Zavarin, M., Zhao, P., and Kersting, A. B., 2011. Stabilization of Plutonium Nano-Colloids by Epitaxial Distortion on Mineral Surfaces. *Environmental Science & Technology* **45**, 2698-2703.

Romanchuk, A. Y., Kalmykov, S. N., and Aliev, R. A., 2011. Plutonium sorption onto hematite colloids at femto- and nanomolar concentrations. *Radiochimica Acta* **99**, 137-144.

Sanchez, A. L., Murray, J. W., and Sibley, T. H., 1985. THE ADSORPTION OF PLUTONIUM-IV AND PLUTONIUM-V ON GOETHITE. *Geochimica Et Cosmochimica Acta* **49**, 2297-2307.

Schwertmann, U. and Cornell, R. M., 2000. Iron oxides in the laboratory, *Iron Oxides in the Laboratory*. Wiley-VCH Verlag GmbH.

Zhao, P. H., Begg, J. D., Zavarin, M., Tumey, S. J., Williams, R., Dai, Z. R. R., Kips, R., and Kersting, A. B., 2016. Plutonium(IV) and (V) Sorption to Goethite at Sub-Femtomolar to Micromolar Concentrations: Redox Transformations and Surface Precipitation. *Environmental Science & Technology* **50**, 6948-6956.